

## Observation of the weak electronic correlations in $\text{KFeCoAs}_2$ ( $3d^6$ ): an isoelectronic to the parent compounds of 122 series of iron pnictides $\text{BaFe}_2\text{As}_2$

This content has been downloaded from IOPscience. Please scroll down to see the full text.

2017 J. Phys.: Condens. Matter 29 085503

(<http://iopscience.iop.org/0953-8984/29/8/085503>)

View [the table of contents for this issue](#), or go to the [journal homepage](#) for more

Download details:

IP Address: 128.42.187.27

This content was downloaded on 10/03/2017 at 23:32

Please note that [terms and conditions apply](#).

You may also be interested in:

[Orbital characters and electronic correlations in  \$\text{KCo}\_2\text{Se}\_2\$](#)

Z H Liu, Y G Zhao, Y Li et al.

[Angle-resolved photoemission spectroscopy study on iron-based superconductors](#)

Ye Zi-Rong, Zhang Yan, Xie Bin-Ping et al.

[Electronic structure of optimally doped pnictide  \$\text{Ba}\_{0.6}\text{K}\_{0.4}\text{Fe}\_2\text{As}\_2\$ : a comprehensive angle-resolved photoemission spectroscopy investigation](#)

H Ding, K Nakayama, P Richard et al.

[Electronic structure and superconductivity of FeSe-related superconductors](#)

Xu Liu, Lin Zhao, Shaolong He et al.

[Electronic structure of  \$\text{Eu}\(\text{Fe}\_{0.79}\text{Ru}\_{0.21}\)\_2\text{As}\_2\$  studied by angle-resolved photoemission spectroscopy](#)

M Xia, W H Jiao, Z R Ye et al.

[Photoemission study of iron-based superconductor](#)

Liu Zhong-Hao, Cai Yi-Peng, Zhao Yan-Ge et al.

[Low-energy microscopic models for iron-based superconductors: a review](#)

Rafael M Fernandes and Andrey V Chubukov

[Calculation of the specific heat of optimally K-doped  \$\text{BaFe}\_2\text{As}\_2\$](#)

Hyungju Oh, Sinisa Coh and Marvin L Cohen

[A flat band at the chemical potential of a  \$\text{Fe}\_{1.03}\text{Te}\_{0.94}\text{S}\_{0.06}\$  superconductor observed by angle-resolved photoemission spectroscopy](#)

P Starowicz, H Schwab, J Goraus et al.

# Observation of the weak electronic correlations in $\text{KFeCoAs}_2$ ( $3d^6$ ): an isoelectronic to the parent compounds of 122 series of iron pnictides $\text{BaFe}_2\text{As}_2$

Z H Liu<sup>1,2</sup>, A N Yaresko<sup>3</sup>, Y Li<sup>4</sup>, P C Dai<sup>4</sup>, H Zhang<sup>5</sup>, B Büchner<sup>1,6</sup>, C T Lin<sup>3</sup> and S V Borisenko<sup>1</sup>

<sup>1</sup> Institute for Solid State Research, IFW Dresden, D-01171 Dresden, Germany

<sup>2</sup> State Key Laboratory of Functional Materials for Informatic, SIMIT, Chinese Academy of Sciences, Shanghai 200050, People's Republic of China

<sup>3</sup> Max Planck Institute for Solid State Research, D-70569 Stuttgart, Germany

<sup>4</sup> Department of Physics and Astronomy, Rice University, Houston, TX 77005-1827, USA

<sup>5</sup> Shanghai Institute of Ceramics, Chinese Academy of Sciences, Shanghai 200050, People's Republic of China

<sup>6</sup> Institute for Solid State Physics, Technology University of Dresden, D-01171 Dresden, Germany

E-mail: [liuzhonghao17@163.com](mailto:liuzhonghao17@163.com) and [s.borisenko@ifw-dresden.de](mailto:s.borisenko@ifw-dresden.de)

Received 14 September 2016, revised 16 December 2016

Accepted for publication 19 December 2016

Published 12 January 2017



CrossMark

## Abstract

Using the angle-resolved photoemission spectroscopy and band structure calculations we study the electronic structure of  $\text{KFeCoAs}_2$ , which is isoelectronic to the parent material of 122 series of iron-based superconductors  $\text{BaFe}_2\text{As}_2$ . Although band structure calculations predict nearly identical dispersions of the electronic states in both compounds, experiment reveals drastic differences in both the global renormalization and Fermi surfaces. On the basis of the comparison of electronic structures of these two isoelectronic compounds, we demonstrate local magnetic correlations as a vital role for the peculiar low-energy electron dynamics of iron-based superconductors.

Keywords: electronic correlations, bands structure, renormalization,  $\text{KFeCoAs}_2$

(Some figures may appear in colour only in the online journal)

## 1. Introduction

Electronic structure of a compound which gives rise to the whole series of superconductors by varying its charge carriers' concentration or under pressure can be vitally important for understanding the mechanism of pairing itself. In the case of cuprates, the Mott-insulating ground state of the parent non-superconducting materials inspired theorists to describe high-temperature superconductivity as originating from such a strongly correlated state of matter. In several families of iron-based superconductors (IBS) the parent members are not superconductors as well, but they are not insulators either. Heated debates as for the degree of correlations in IBS are

not over until now [1–3]. From one side IBS are itinerant metals which are reasonably well described by the local density approximation (LDA) band structure calculations, from another—they are antiferromagnets with strongly, sometimes up to the order of magnitude, renormalized low-energy dispersions. Although it became possible to describe the renormalization qualitatively in terms of Hund's rule coupling using the dynamical mean-field theory (DMFT) [4, 5] or phenomenologically in terms of self-energy using the angle-resolved photoemission spectroscopy (ARPES) [6], many puzzling features remain unexplained. Significant departure of the experimental Fermi surfaces [7–10] from the ones predicted by LDA cannot be explained in terms of global renormalization

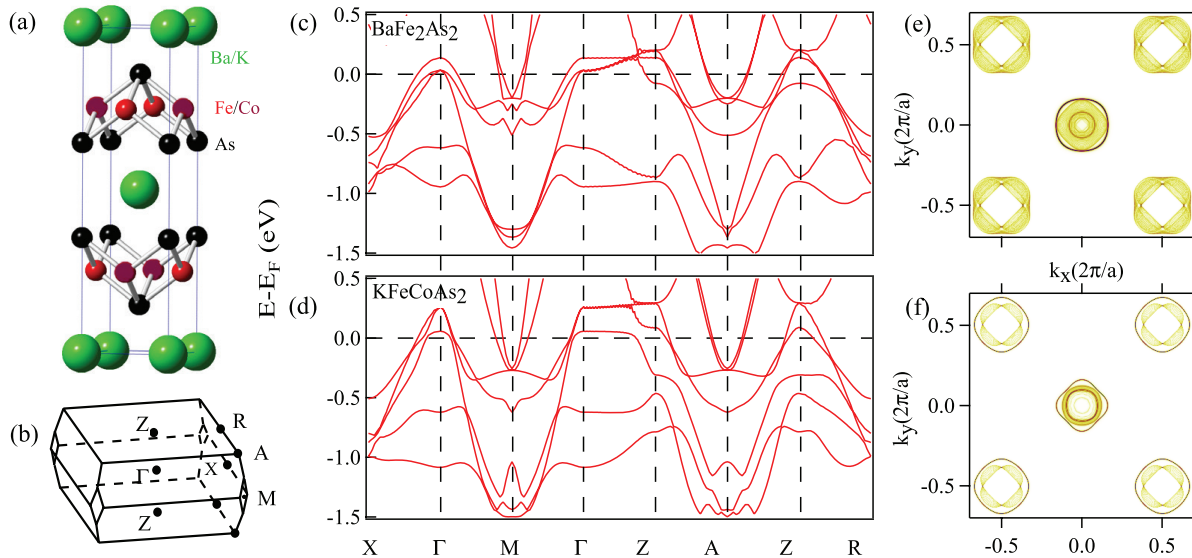


**Figure 1.** (a) Crystal structure of  $\text{BaFe}_2\text{As}_2/\text{KFeCoAs}_2$  used in the calculations. Due to Co-substitution, we present half-to-half Fe (red) and Co (dark) atoms in the lattice. (b) Schematic Brillouin zone (BZ) of the materials. (c) and (d) Calculated band structures of  $\text{BaFe}_2\text{As}_2/\text{KFeCoAs}_2$  along high symmetry lines near the Fermi level ( $E_F$ ). (e) and (f) Calculated Fermi surfaces of  $\text{BaFe}_2\text{As}_2/\text{KFeCoAs}_2$ .

by a single factor, as most of the theories of correlated electrons would prescribe. A number of robust experimental facts point to strong orbital-dependence of such renormalization [10–15]. In FeSe, for instance, renormalization of  $xy$ -band is of the order of 9 while the rest of the bands are only three times narrower [10]. Even if such orbital dependent renormalization is captured by theory, but still considered as squeezing of the bands towards the Fermi level ( $E_F$ ), it would leave the theoretical Fermi surface intact, i.e. it would not be sufficient to explain the experimental Fermi surfaces. The reason for this discrepancy is due to the energy shift of the opposite sign of the dispersion curves corresponding to the center and the corner of the Brillouin zone (BZ): ‘blue shift’ of the states close to the center of the BZ and ‘red shift’ of the states in the corners of the BZ, counting from  $E_F$ . The microscopic understanding of such shifts is still absent. Moreover, the renormalization factor seems to vary by up to an order of magnitude when comparing members of the IBS families and very closely related materials [16–18]. Whether the shifts and large scale bandwidth renormalization are related is therefore the question of fundamental importance. In order to address it, we studied isoelectronic to  $\text{BaFe}_2\text{As}_2$  material with the chemical formula  $\text{KFeCoAs}_2$  by means of angle-resolved photoemission and band-structure calculations.

The 122 family is a good candidate to study the electronic correlations in IBS, due to both electrons ( $\text{Ba}(\text{Fe}_{1-x}\text{Co}_x)_2\text{As}_2$ ) and holes ( $\text{Ba}_{1-x}\text{K}_x\text{Fe}_2\text{As}_2$ ) doping can suppress magnetic order and lead to a dome of superconductivity before a more conventional metal is reached [19, 20]. We have selected  $\text{KFeCoAs}_2$  ( $3d^6$ ) since it represents a very interesting modification of the parent 122 compound: half of the iron atoms are replaced by Co atoms, which would dope the systems by electrons significantly, but Ba atoms are replaced by K atoms, exactly compensating the electron doping caused by Co atoms. Previous theoretical and experimental study of 122 series revealed that the number of  $3d$  electrons was a dominating influence in the

electronic correlations, the bands structure and the Fermi surfaces. For one thing, the strength of electronic correlations is efficiently tuned by changing the filling of the  $3d$  electrons [3, 21]. In this principle, the two similar compounds would have more or less similar strength of electronic correlations. For another thing, In  $\text{BaFe}_2\text{As}_2$ , the pairing interaction and thus superconductivity are enhanced by the nesting between the hole and electron pockets which are connected by the antiferromagnetic wavevectors [7, 11]. The electronic order dictated by the nesting instability and the static magnetic order developed at the low temperature have grown to be generally accepted in IBS. The calculations in  $\text{KFeCoAs}_2$  suggest that the Fermi surface and electronic structure are rather similar to those of  $\text{BaFe}_2\text{As}_2$ , but is less magnetic [22]. While so far there are no experimental reports on the low-energy electronic dispersions of  $\text{KFeCoAs}_2$ .

In this work, we present the Fermi surface and band structure of  $\text{KFeCoAs}_2$ , and demonstrate that the renormalization is virtually absent in  $\text{KFeCoAs}_2$  and so are the ‘shifts’ in comparison with  $\text{BaFe}_2\text{As}_2$ . Our results suggest the intimate relation between these two robust experimental observations and, as a consequence, to an important influence of local magnetic correlations in the physics of IBS.

## 2. Methods

High quality single crystals of  $\text{KFeCoAs}_2$  ( $T_c = 0$ , non-magnetic), and  $\text{BaFe}_2\text{As}_2$  were synthesized by the flux method [23, 24]. Samples with size smaller than  $1 \times 1 \text{ mm}^2$  were cleaved *in situ*, yielding a flat mirror like (001) surfaces. ARPES measurements were performed at ‘1-cubed’ end-station in BESSY and at ‘dreamline’ end-station in SSRF, within the range of photon energies (50–130 eV) and various polarizations. The overall energy and momentum resolutions were set to  $\sim 3$ –15 meV and  $\sim 0.013 \text{ \AA}^{-1}$ . During the measurements, the pressure was maintained better than  $5 \times 10^{-11}$  Torr.

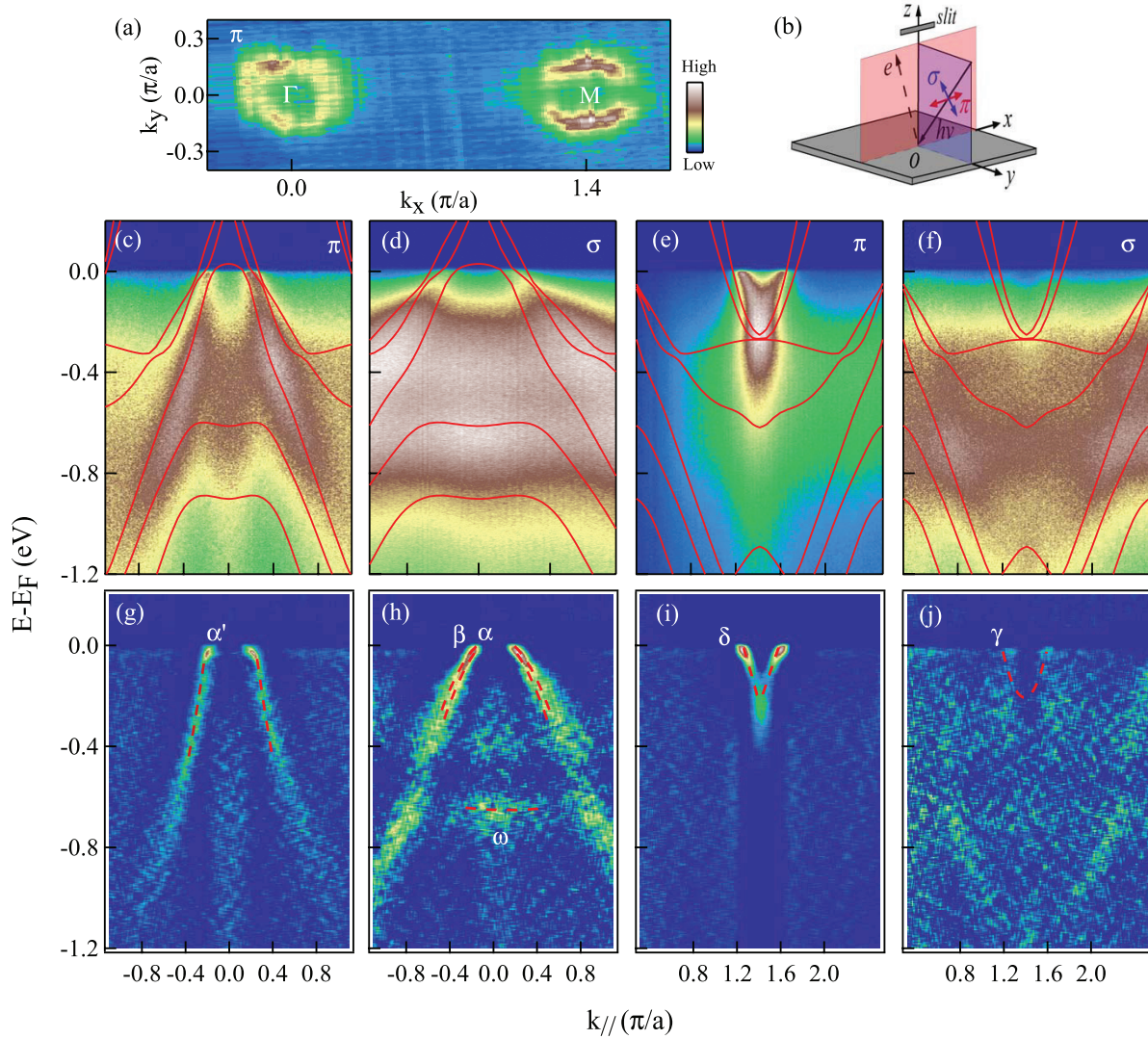


**Figure 2.** (a) Photoemission intensity map of KFeCoAs<sub>2</sub> integrated at  $E_F$  ( $\pm 10$  meV). (b) Sketch of the experimental polarization setup. The  $\pi$ ( $\sigma$ ) geometry refers to the electric fields of the incident photons within (normal to) the mirror plane (pink). We note that our experimental setup for the  $\sigma$  geometry includes a polarization component along  $z$ . (c) and (d) Intensity plots of band dispersion at  $\Gamma$  point along  $\Gamma M$  direction in  $\pi$  and  $\sigma$  geometries respectively. (e) and (f) Corresponding to (c) and (d) respectively, but taken at the M point. (g)–(j) The second derivative plots corresponding to (c)–(f). The solid lines in (c)–(f) are un-renormalized LDA-calculated band structures. The dashed lines in (g)–(j) are guides to the eye for the band dispersions. All the data were taken at 1 K with 80 eV photons ( $k_z \sim 0.67\pi/c$ ).

Band structure calculations were performed based on the LDA with the experimental crystal structural parameters  $a = 3.838$  Å,  $c = 13.709$  Å for KFeCoAs<sub>2</sub>, and  $a = 3.962$  Å,  $c = 13.167$  Å for BaFe<sub>2</sub>As<sub>2</sub> respectively [23]. The internal coordinates  $z_{As}$  were relaxed by energy minimization for ordered cells. Half-to-half Fe and Co atoms in KFeCoAs<sub>2</sub> cause the existence of the superlattice here. The crystal structure of KFeCoAs<sub>2</sub> and BaFe<sub>2</sub>As<sub>2</sub> used in the calculations and the corresponding 3D BZ are shown in figures 1(a) and (b) respectively.

### 3. Results and analysis

As is seen from the results of the calculations along the high-symmetry directions in figures 1(c) and (d), the electronic structures are nearly identical with some moderate discrepancies along the  $\Gamma Z$  direction. Indeed, the low-energy electron

dynamics in these systems is defined by  $3d$  electrons and the only principal difference is that the half of these  $3d$  electrons in the case of KFeCoAs<sub>2</sub> stems from Co-atom. Apparently, this is not a significant variation from the point of view of the LDA theory [22]. As for the contribution of Ba and K states, they do not define the structure near  $E_F$  as is anticipated for the atoms from the interstitial blocks, mostly acting as charge reservoirs [25]. The Fermi surfaces also look very similar, as shown in figures 1(e) and (f), both suggesting a high degree of nesting between the hole-like sheets in the center of the BZ and electron-like sheets in its corners.

We present our ARPES results taken from KFeCoAs<sub>2</sub> single crystals and compare them with LDA results in figure 2. The Fermi surface map (figure 2(a)) remarkably reproduces the LDA result. There are at least two well discernible pockets centered at the zone center and corners of similar size and shape, i.e. reasonably well nested. Figures 2(c)–(f) and

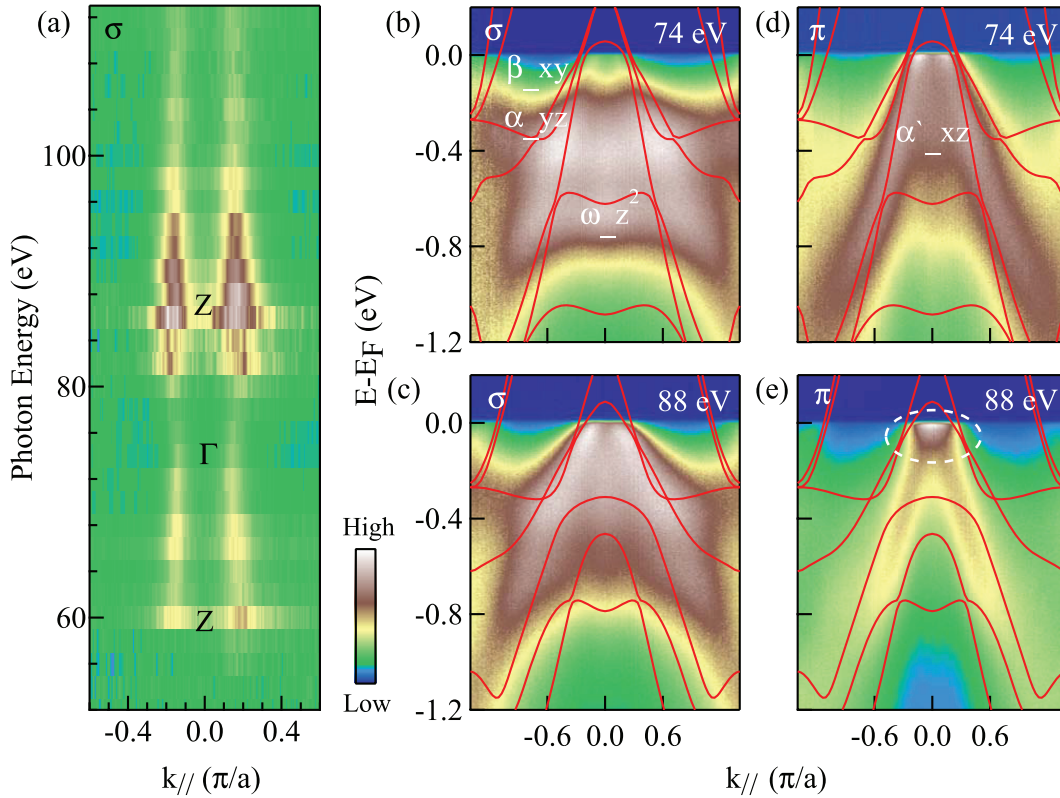


**Figure 3.** (a) Intensity plot in the  $k_z - k_{//}$  plane at  $E_F (\pm 10 \text{ meV})$  of  $\text{KFeCoAs}_2$  in  $\sigma$  geometry. (b) and (c) Intensity plots of band dispersion at the BZ center in  $\sigma$  geometry, taken at 1 K with 74 ( $\Gamma$  point) and 88 eV (Z point) photons respectively. (d) and (e) Corresponding to (b) and (c) respectively, but taken in  $\pi$  geometry. The solid lines in (b)–(e) are un-renormalized LDA-calculated band structures. The white circle in (e) indicates a hot spot formed by the top of  $\alpha'$  band.

(g)–(j) show the intensity plots representing the distribution of ARPES intensity as a function of energy and momentum and the corresponding the second derivative plots, respectively. In order to determine the orbital composition of the observed states, we have recorded these datasets in different geometries. Our experimental setup is shown in figure 2(b).  $\pi(\sigma)$  geometry refers to the electric fields of the incident photons within (normal to) the mirror plane. The even (odd) orbitals with respect to the mirror plane are detected in  $\pi(\sigma)$  geometry. At the  $\Gamma$  point, it unambiguously allows us to attribute  $d_{xz}/d_{yz}$  states to the  $\alpha'$  and  $\alpha$  bands, while the  $\beta$  band is formed by  $d_{xy}$  states. The  $\omega$  band is noticeably enhanced in  $\sigma$  geometry having the  $z$ -component polarization and thus corresponding to  $d_{z^2}$  character. At the  $M$  point, the  $\delta$  and  $\gamma$  bands are highlighted in  $\pi$  and  $\sigma$  geometry respectively, suggesting that  $\delta$  is of  $d_{xz}$ , and  $\gamma$  is of  $d_{yz}$  or  $d_{xy}$  orbital character. The general agreement with LDA band structure is very good also for these datasets. Comparing the energy scales of experiment and calculations one can extract the renormalization of the above discussed dispersing states: the  $\alpha'$ ,  $\alpha$ ,  $\beta$ ,  $\delta$ , and  $\gamma$  bands are renormalized by the factor of 1, 1, 1.2, 1.2, and 1.2 respectively. These factors are much lower than the usual band narrowing in others 122-materials [10–18, 26] and emphasize the suitability for the LDA description of the studied material.

It is known that the IBS cannot be perfectly approximated by quasi-2D models. A considerable degree of  $k_z$  dispersion is predicted by the calculations. Therefore, it is important to investigate the electronic structure as a function of  $k_z$  as well.

We have done this using usual ARPES methodology of scanning photon energies. The intensity map representing the cut of the Fermi surface by the  $k_z - k_{//}$  plane is shown in figure 3(a). We have observed periodic variations of the distance between the most pronounced crossings near the zone center and in such a way determined high-symmetry points along  $k_z$ . In figures 3(b)–(e), we present the cuts along  $\Gamma M$  (74 eV) and  $ZA$  (88 eV) directions respectively and append the corresponding un-renormalized LDA results on them. The degree of  $k_z$  dispersion is indeed considerable and is in a close agreement with the calculations. As in the case of other pnictides [27], according to the calculations, there is a 3D Fermi surface supported by  $\alpha'$ -dispersion, which sinks below  $E_F$  for certain  $k_z$ -values (see the crossing along the  $\Gamma Z$ -direction in figure 1(d)). The experimental data likewise reveal the 3D character of  $\alpha'$ . This is seen by comparing figures 3(d) and (e). However, at Z point,  $\alpha'$  does not shift down so much, and forms a hot spot at  $E_F$ , as shown in figure 3(e). This apparent discrepancy with LDA calculations is probably due to the finite  $k_z$  resolution of our experiment. The 3D FS is formed partially by  $d_{z^2}$  states which strongly disperse along  $\Gamma Z$  direction [27].

Having studied the electronic structure of  $\text{KFeCoAs}_2$  in details, we can now compare it with that of  $\text{BaFe}_2\text{As}_2$  directly. The electronic structure of  $\text{BaFe}_2\text{As}_2$  has been extensively studied by many ARPES [7, 28–32]. Here we present only the key datasets. It is known that the parent 122 undergoes a SDW transition at approximately 142 K [33]. Therefore its ground state would correspond to this antiferromagnetic state

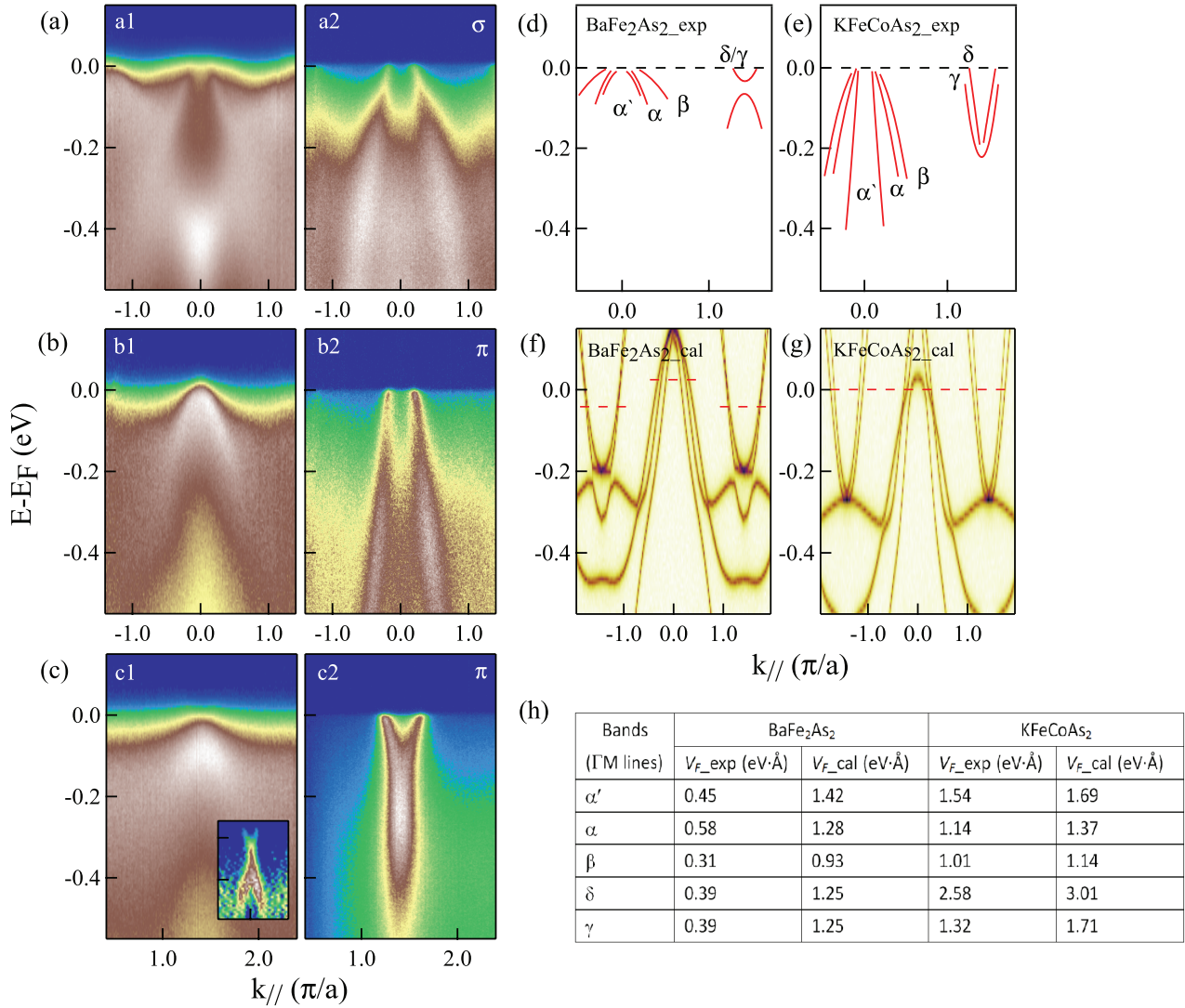


**Figure 4.** Comparisons of the low-energy band structures between BaFe<sub>2</sub>As<sub>2</sub> (150 K, 80 eV) and KFeCoAs<sub>2</sub> (1 K, 80 eV). (a) At the zone center in  $\sigma$  geometry. (a1) and (a2) Intensity plot of band dispersion of BaFe<sub>2</sub>As<sub>2</sub>/KFeCoAs<sub>2</sub>. (b) Corresponding to (a), but taken in  $\pi$  geometry. (c) Corresponding to (b), but taken at the zone corner. The second derivative plot of the electron pocket is inserted. (d) and (e) Abstracted bands structure from experiments on BaFe<sub>2</sub>As<sub>2</sub> and KFeCoAs<sub>2</sub> respectively. (f) and (g) LDA results of BaFe<sub>2</sub>As<sub>2</sub> and KFeCoAs<sub>2</sub> respectively. The shades of bands indicate some components of the  $k_z$  distribution. (h) Table of measured ( $V_{F\_exp}$ ) and calculated ( $V_{F\_cal}$ ) Fermi velocities of BaFe<sub>2</sub>As<sub>2</sub> and KFeCoAs<sub>2</sub> along  $\Gamma$ M lines. The error bars of  $V_{F\_exp}$  are less than 0.02. The  $V_{F\_cal}$  is taken from  $k_z \sim 0.67\pi/c$  (80 eV) in calculations.

with the folded BZ. To avoid possible complications we compare the data taken above SDW transition temperature when the system is in the paramagnetic state. In figures 4(a)–(c), we present such data for the high-symmetry cuts running through the  $\Gamma$  and  $M$  points and compare them with the similar datasets recorded from KFeCoAs<sub>2</sub> using the same photon energy (80 eV). One can clearly see that most of the  $t_{2g}$  bands near  $E_F$  in BaFe<sub>2</sub>As<sub>2</sub> are ‘squeezed’ in the range of 0.2 eV below  $E_F$  as observed in [28–32]. While in KFeCoAs<sub>2</sub>, the similar features stretch down to 0.4 eV below  $E_F$ , or even lower, as abstracted experimental data shown in figures 4(d) and (e). The squeezed bands in BaFe<sub>2</sub>As<sub>2</sub> obviously result from much stronger electronic correlations in comparison with KFeCoAs<sub>2</sub>. Indeed, the Fermi velocities of the features near the  $\Gamma$  point in BaFe<sub>2</sub>As<sub>2</sub> are 0.45, 0.58, and 0.31 eV·Å for the  $\alpha'$ ,  $\alpha$ , and  $\beta$  bands respectively. The electron pocket dispersions have an

equivalent Fermi velocity of 0.39 eV·Å. All of them are much smaller than LDA-calculated data. While in KFeCoAs<sub>2</sub>, the Fermi velocities of the  $\alpha'$ ,  $\alpha$ ,  $\beta$ ,  $\delta$ , and  $\gamma$  bands are 1.54, 1.14, 1.01, 2.58, and 1.32 eV·Å respectively, which are close to the LDA predictions. The measured and calculated Fermi velocities of the two compounds are listed in figure 4(h). Apart from different renormalizations, the dramatic dichotomy between the mutual positions of the band extrema and  $E_F$  is clearly present: in BaFe<sub>2</sub>As<sub>2</sub> the tops of the bands near  $\Gamma$  point are shifted down in energy whereas the construct in the corner of the BZ is moved up in accordance with mentioned above ‘shift’ universally present in all IBS. While in KFeCoAs<sub>2</sub>, the calculated bands structure good fit to the experimental data without any ‘shifts’. We plot the positions of the experimental  $E_F$  as red dashed lines in figure 4(f) to emphasize the presence of such a shift in parent 122 material.

#### 4. Discussion

Why are the experimental electronic structures of the two very similar materials that different? Moreover, this difference is not formal being expressed in their physical properties. One is a strongly correlated antiferromagnet giving rise to the whole family of superconductors and the other one suggests a straightforward metal, nicely described by LDA. The only difference from the point of view of itinerant physics is the different atomic origin of one conduction electron: in BaFe<sub>2</sub>As<sub>2</sub> it is taken from interstitial Ba atom whereas in KFeCoAs<sub>2</sub> it is from an in-slab Co atom. The size of the Co atom is only slightly smaller than the Fe atom which is reflected by the size of *ab* lattice constants [34]. As was shown above, LDA solution is not influenced much by all differences mentioned above.

Spatial localization of randomly scattered dopant atom is probably not decisive as well, since IBS are obtained equally effectively either by Fe or interstitial substitution without strongly altering the electronic structure. The case of KFeCoAs<sub>2</sub> is a special one, on account of Co atoms most likely forming a new magnetic sublattice. Local magnetic moment of Co atoms is expected to be significantly smaller than that of iron (1.75 versus 2.78 [34]). Since it is Hund's rule coupling which is responsible for the strong renormalization of the factor of ~3 in IBS [3–5], the current situation is probably dictated by the screening of the exchange interaction due to the presence of this new sublattice of weaker local moments. It is remarkable that also the blue and red shifts of the band structure elements are gone in KFeCoAs<sub>2</sub>. Additional, Hund's *J* decouples the charge excitations in the different orbitals, so the system shows orbital-dependent correlation effects. As one of the main proposals of pairing mechanisms in IBS, superconducting pairing is dominated by As-bridged local antiferromagnetic super-exchange interactions. The Fe *d*<sub>xy</sub> orbital is prominent in this picture [26, 35–37]. Thus the famous distortion of the Fermi surface when both hole-like and electron-like FSs become smaller in the experiment is possible due to orbital dependent renormalization, which is can be also caused by magnetic interaction of local character. Considering all IBS share this peculiarity, at least qualitatively, the Hund's rule coupling seems to be an essential ingredient of superconductivity.

#### 5. Conclusions

In summary, we have studied the electronic structure of KFeCoAs<sub>2</sub> by means of ARPES and found that it is well

described by the LDA approach. Comparison with the isoelectronic parent 122 material BaFe<sub>2</sub>As<sub>2</sub> demonstrated that both, the global renormalization and the Fermi surface change are due to the reduced electronic correlations, which is seriously affected by the local magnetic interactions.

#### Acknowledgments

This project was supported by the German Science Foundation under Grants No. BO 1912/2-2 within SPP 1458, Shanghai Province Science Foundation and National Natural Science Foundation of China.

#### References

- [1] Qazilbash M M *et al* 2009 *Nat. Phys.* **5** 647
- [2] Wang W L *et al* 2009 *Phys. Rev. B* **80** 014508
- [3] Medici L *et al* 2014 *Phys. Rev. Lett.* **112** 177001
- [4] Yin Z P *et al* 2011 *Nat. Mater.* **10** 932
- [5] Werner P *et al* 2012 *Nat. Phys.* **8** 331
- [6] Evtushinsky D *et al* 2014 (arXiv:1409.1537)
- [7] Zabolotnyy V *et al* 2009 *Nature* **457** 569
- [8] Borisenko S *et al* 2010 *Phys. Rev. Lett.* **105** 067002
- [9] Maletz J *et al* 2013 *Phys. Rev. B* **88** 134501
- [10] Maletz J *et al* 2014 *Phys. Rev. B* **89** 220506
- [11] Ding H *et al* 2011 *J. Phys.: Condens. Matter* **23** 135701
- [12] Brouet V *et al* 2011 (arXiv:1105.5604v1)
- [13] Yi M *et al* 2013 *Phys. Rev. Lett.* **110** 067003
- [14] Yoshida T *et al* 2014 *Front. Phys.* **2** 17
- [15] Charnukha A *et al* 2015 *Sci. Rep.* **5** 10392
- [16] Xu N *et al* 2013 *Phys. Rev. X* **3** 011006
- [17] Liu Z H *et al* 2015 *J. Phys.: Condens. Matter* **27** 295501
- [18] Fan Q *et al* 2015 *Phys. Rev. B* **91** 125113
- [19] Suzuki S *et al* 2010 *Phys. Rev. B* **82** 184510
- [20] Goltz T *et al* 2014 *Phys. Rev. B* **89** 144511
- [21] Werner P *et al* 2008 *Phys. Rev. Lett.* **101** 166405
- [22] Singh D 2009 *Phys. Rev. B* **79** 174520
- [23] Lv B 2009 *PhD Dissertation* Faculty of the Department of Chemistry, University of Houston, Houston, TX
- [24] Rotter M *et al* 2008 *Phys. Rev. Lett.* **101** 107006
- [25] Liu Z H *et al* 2015 *App. Phys. Lett.* **106** 052602
- [26] Liu Z H *et al* 2012 *Phys. Rev. Lett.* **109** 037003
- [27] Borisenko S *et al* 2016 *Nat. Phys.* **12** 311
- [28] Fink J *et al* 2009 *Phys. Rev. B* **79** 155118
- [29] Yang L X *et al* 2009 *Phys. Rev. Lett.* **102** 107002
- [30] Yi M *et al* 2011 *Proc. Natl Acad. Sci.* **108** 6878–83
- [31] Richard P *et al* 2010 *Phys. Rev. Lett.* **104** 137001
- [32] Liu C *et al* 2010 *Nat. Phys.* **6** 419
- [33] Huang Q *et al* 2008 *Phys. Rev. Lett.* **101** 257003
- [34] Galperin F 1973 *Phys. Status Solidi* **57** 715
- [35] Ma F J *et al* 2008 *Phys. Rev. B* **78** 224517
- [36] Hu J P *et al* 2012 *Sci. Rep.* **2** 381
- [37] Yang F *et al* 2013 *Phys. Rev. B* **88** 100504